



1 Oxidative potential in rural, suburban and city centre atmospheric 2 environments in Central Europe

3 Máté VÖRÖSMARTY¹, Gaëlle UZU², Jean-Luc JAFFREZO², Pamela DOMINUTTI²,
4 Zsófia KERTÉSZ³, Enikő PAPP³, and Imre SALMA⁴

5 ¹Hevesy György Ph. D. School of Chemistry, Eötvös Loránd University, Budapest, Hungary

6 ²University of Grenoble Alps, IRD, CNRS, INRAE, Grenoble, France

7 ³Laboratory for Heritage Science, Institute for Nuclear Research, Debrecen, Hungary

8 ⁴Institute of Chemistry, Eötvös Loránd University, Budapest, Hungary

9 *Correspondence to:* Imre Salma (salma.imre@ttk.elte.hu)

10 **Abstract.** Oxidative potential (OP) is an emerging health-related metric which integrates several
11 physicochemical properties of particulate matter (PM) that are involved in the pathogenesis of the diseases
12 resulting from the exposure to PM. Daily PM_{2.5}-fraction aerosol samples collected in the rural background
13 of the Carpathian Basin and in the suburban area and centre of its largest city of Budapest in each season
14 over one year were utilised to study the OP at the related locations for the first time. The samples were
15 analysed for particulate matter mass, main carbonaceous species, levoglucosan and 20 chemical elements.
16 The resulted data sets were subjected to positive matrix factorisation to derive the main aerosol sources.
17 Biomass burning (BB), suspended dust, road traffic, oil combustion, vehicle metal wear and mixed
18 industrial source were identified. The OP of the sample extracts in simulated lung fluid was determined
19 by ascorbic acid (AA) and dithiothreitol (DTT) assays. The comparison of the OP data sets revealed some
20 differences in the sensitivities of the assays. In the heating period, both the OP and PM mass levels were
21 higher than in spring and summer, but there was a clear misalignment between them. In addition, the
22 heating period-to-non-heating period OP ratios in the urban locations were larger than for the rural
23 background by factors of 2–4. The OP data sets were attributed to the main aerosol sources using multiple
24 linear regression with the weighted least squares approach. The OP was unambiguously dominated by
25 BB at all sampling locations in winter and autumn. The joint effects of motor vehicles involving the road
26 traffic and vehicle metal wear played the most important role in summer and spring, with considerable
27 contributions from oil combustion and resuspended dust. In winter, there is temporal coincidence between
28 the most severe daily PM health limit exceedances in the whole Carpathian Basin and the chemical PM
29 composition causing larger OP. Similarly, in spring and summer, there is a spatial coincidence in
30 Budapest between the urban hotspots of OP-active aerosol constituents from traffic and the high population
31 density in central quarters. These features offer possibilities for more efficient season-specific air quality
32 regulations focusing on selected aerosol sources rather than on PM mass in general.



33 **1 Introduction and objectives**

34 Poor air quality caused by high concentrations of particulate matter (PM) is one of the most severe public
35 health concerns for humans worldwide (e.g. Lelieveld et al., 2015, 2020; Bondy, 2016; Cohen et al.,
36 2017). Its acute and chronic effects, such as lung, cardiovascular and cerebrovascular diseases have been
37 documented in both epidemiological and toxicological studies (e.g. Donaldson et al., 2005; Valavanidis
38 et al., 2008; Apte et al., 2015; Riediker et al., 2019; Kelly and Fussell, 2020).

39

40 Due to the chemical, physical and biological complexity of ambient aerosol particles, their dynamic
41 character and possible synergisms among air pollutants, a sophisticated interplay of multiple factors is
42 involved in the pathogenesis of the diseases resulting from the exposure to PM. The main factors can
43 involve: 1) mass concentrations of PM_{2.5} or PM₁₀ size fractions, 2) amounts of potentially toxic chemical
44 components such as transition and heavy metals, polycyclic aromatic hydrocarbons (PAHs), soot and
45 specific organics, 3) certain chemical speciation forms such as Cr(VI) versus Cr(III), 4) lung
46 bioaccessibility of critical constituents, 5) surface reactivity of particles, 6) number concentrations of very
47 small particles such as ultrafine particles or engineered nanomaterials, 7) shape and morphology of
48 particles such as for asbestos or silica and 8) active components of biogenic origin such as bacteria,
49 viruses, pollens and moulds or with radioactivity such as radon progeny. Therefore, it cannot be expected
50 that a single or a few aerosol metrics broadly express the induced biological responses. In the first
51 approximation, PM mass is often selected from these factors as a simplistic metric, and it can be refined
52 by further particle properties.

53

54 One of the most important biological mechanisms by which PM induces adverse health effects is causing
55 an oxidant-antioxidant imbalance in the respiratory system at the cellular level (Kelly and Mudway, 2003;
56 Borm et al., 2007; Kelly and Fussell, 2012, 2015; Cassee et al., 2013; Valavanidis et al., 2013). This is
57 called as oxidative stress. It is related to 1) stimulating cells to uncontrolled production of excess reactive
58 oxygen species (ROS) endogenously, e.g. directly by Fenton-type reactions of redox-active aerosol
59 components in the human body or indirectly through biotransformation, e.g. of PAHs or 2) inefficient
60 elimination of ROS by the antioxidant defence system of the body. These can lead to inflammatory
61 processes that increase the risk for various diseases and can result in biological aging and apoptosis (Ayres
62 et al., 2008; Verma et al., 2012; Gao et al., 2020). The capacity of PM to invoke oxidative stress is
63 quantified by its oxidative potential (OP). This integrates several factors of the particle properties 1–8
64 listed above. Numerous epidemiological studies suggest that the OP can be one of the central quantities
65 that is responsible for specific acute health effects such as emergency treatment of asthma and congestive



66 heart failure and that largely explains the underlying biological bases of toxicity (e.g. Bates et al., 2015;
67 Kelly and Fussel, 2015; Abrams et al., 2017; Yue et al., 2018; Daellenbach et al., 2020; Dhalla et al.,
68 2000; Zhang et al., 2022; Baumann et al., 2023).

69

70 As a result, there has been a substantial and increasing scientific interest in the measurement
71 improvements of OP using (biological) in vivo, in vitro cellular and in vitro acellular assays, and in the
72 identification of the aerosol components and sources closely related to OP (e.g. Cho et al., 2005; Künzli
73 et al., 2006; Boogaard et al., 2012; Verma et al., 2014, 2015; Kelly and Fussel, 2015; Fang et al., 2016;
74 Calas et al., 2017; Weber et al., 2018; Shahpoury et al., 2021; Borlaza et al., 2021b, 2022; Lionetto et al.,
75 2021; Zhang et al., 2022). The OP is frequently measured by acellular assays for exogenous ROS, in
76 which the PM extract or the particles directly cause a consumption rate of some antioxidants such as
77 ascorbic acid (AA) or of some chemical surrogates to cellular reducing agents, e.g. dithiothreitol (DTT).
78 The quantifications are generally based on spectrophotometry. More sophisticated detection methods
79 which directly determine the ROS production are also available (Katerji et al., 2019).

80

81 The most frequently used assays were compared for PM₁₀-fraction aerosol samples considering the
82 chemical composition of particles as well (Calas et al., 2018; Lionetto et al., 2021). It was concluded that
83 the assays strongly correlated with each other but were not equivalent. All assays were somewhat specific,
84 and no consensus has been reached on the “best assay” nor on a standardised methodology for each assay
85 (Weber et al., 2021; Zhang et al., 2022).

86

87 The main common features of the assays are that 1) they exhibit different responses to various groups of
88 ROS-generating compounds and their bioavailability, 2) their sensitivity depends on the partner reaction
89 compound to ROS, and 3) they show nonlinear response to PM mass concentration (Charrier et al., 2016;
90 Fang et al., 2016; Calas et al., 2017; Shahpoury et al., 2021). A large number of PM constituents were
91 identified to influence the OP. The DTT assay responds sensitively to ROS produced by organic
92 compounds and indirectly by soluble transition metals, mainly Cu(II), Mn(II) and Fe(II), and can be also
93 influenced by synergetic or antagonistic effects between some chemical components (Charrier and
94 Anastasio, 2012; Bates et al., 2019; Shahpoury et al., 2021; Borlaza et al., 2022). The AA assay was
95 shown to express large sensitivity to transition metals and some specific organics such as quinones
96 (Künzli et al., 2006; Godri et al., 2011; Visentin et al., 2016).

97

98 It is important to extend the studies on this emerging health-related metric to cities and regions in the
99 world. The knowledge on the OP for a large part of Central Europe, namely the Carpathian Basin, is



100 deficient or missing (Szigeti et al., 2015). The major objective of this study was to present, discuss and
101 interpreted the OP data determined by AA and DTT assays in PM_{2.5}-fraction aerosol samples collected in
102 parallel in central Budapest, its suburban area and rural background within the Carpathian Basin in each
103 season over one year. We also investigated the spatiotemporal dependencies, and identified the main
104 aerosol sources of OP. The study can contribute to our general knowledge on the OP as well.

105 **2 Methods**

106 **2.1 Sample collections**

107 The samplings in the rural background were performed at the K-puszta station (N 46° 57' 56", E 19° 32'
108 42", 125 m above sea level, a.s.l.), which represents the main plain part of the basin (Salma et al., 2020a).
109 Budapest, with ca. 2.2 million inhabitants in the metropolitan area, is the largest city in the region. Its
110 suburban environment was characterised by collections at the Marczell György Main Observatory (N 47°
111 25' 46", E 19°10' 54", 138 m a.s.l.) of the Hungarian Meteorological Service (Salma et al., 2022). This is
112 in a southeast residential part of the city. The samplings in the city centre were accomplished at the
113 Budapest platform for Aerosol Research and Training (BpART) Laboratory (N 47° 28' 30", E 19° 03' 45",
114 115 m a.s.l.), which represents an average atmosphere of the city centre (Salma et al., 2016).

115

116 Three identical high-volume sampling devices equipped with PM_{2.5} inlets (DHA-80, Digitel, Switzerland)
117 were deployed at the sites (Salma et al., 2020a). The collection substrates were prebaked quartz fibre
118 filters with a diameter of 150 mm (QR-100, Advantec, Japan). Daily aerosol samples were taken starting
119 at midnight of local time. The samples corresponding to air volumes of 720 m³ were collected in parallel
120 with each other over semi-consecutive days in October 2017 (autumn), January 2018 (winter), April 2018
121 (spring) and July 2018 (summer). The total numbers of the filters were 56 at the rural site, 59 in the
122 suburban area, and 28 in the city centre. The samples evenly spread among the four seasons. In addition,
123 one field blank was taken at each location and in each season. The filters were wrapped in preheated Al
124 foils, sealed in plastic bags and stored at a temperature of <-4 °C until the analyses. The samples represent
125 a gradual transition from the central part of a large continental European city through its suburban area to
126 its regional background in all seasons.

127 **2.2 Analyses and data treatment**

128 Particulate matter mass was determined by gravimetry (Cubis MSA225S-000-DA, Sartorius, Germany,
129 sensitivity of 10 µg). The blank-corrected PM mass data were above the limit of quantitation (LOQ),
130 which was 1 µg m⁻³.



131

132 Filter punches were analysed by thermal-optical transmission method using a laboratory OC/EC analyser
133 (Sunset Laboratory, USA) adopting the EUSAAR-2 thermal protocol (Cavalli et al., 2010). All blank-
134 corrected organic carbon (OC) and elemental carbon (EC) data were above the LOQ, which were 0.38
135 and 0.04 $\mu\text{g m}^{-3}$, respectively. Filter pieces were analysed for levoglucosan (LVG) by gas
136 chromatography–mass spectrometry (Varian 4000, USA) after trimethylsilylation (Blumberger et al.,
137 2019). All blank-corrected LVG data were above the LOQ, which was 1.2 ng m^{-3} .

138

139 Parts of the filters were analysed by particle-induced X-ray emission spectrometry for S, Cl, K, Ca, Ti,
140 V, Cr, Mn, Fe, Co, Ni, Cu, Zn, As, Br, Rb, Sr, Zr, Ba and Pb using an external beam of protons with an
141 energy of 2.35 MeV and a current of 20 nA (Aljboor et al., 2022). The obtained spectra were evaluated
142 by the GUPIXWIN program. The filters were treated as thin layer samples. For S, Cl, K, Ca, the self-
143 absorption effects of quartz filters were corrected for (Chiari et al., 2018).

144

145 Concentrations of EC and OC from fossil fuel combustion and from biomass burning (BB), namely EC_{FF}
146 and OC_{FF} , EC_{BB} and OC_{BB} , respectively and of OC from biogenic sources (OC_{BIO}) were previously
147 estimated by a coupled radiocarbon-LVG marker method (Salma et al., 2020a). Secondary organic carbon
148 (SOC) was also assessed previously using the EC tracer method for primary OC (Salma et al., 2022).
149 These results were used as supplementary data in interpretations.

150 **2.3 Determination of oxidative potential**

151 Specified filter areas were extracted in a simulated human respiratory tract lining fluid solution composed
152 of Gamble's solution with dipalmitoylphosphatidylcholine (DPPC; the major phospholipid of lung
153 surfactant; Calas et al., 2017, 2018). The extractions were carried out by vortex agitation at 37 °C for 1
154 h. The overall procedure represents conditions which are close to the respiratory system. Isoconcentration
155 extracts with 10 $\mu\text{g ml}^{-1}$ of PM mass were obtained for all samples to overcome possible nonlinear OP
156 response of PM concentrations (Charrier and Anastasio, 2012; Calas et al., 2017).

157

158 The OP of the extracts was measured without filtration by two single-compound in vitro acellular assays,
159 i.e. AA and DTT assays. These two methods are widely used for OP determination (e.g. Calas et al., 2018;
160 Daellenbach et al., 2020; Lionetto et al., 2021; Shahpoury et al., 2021). However, there is a fundamental
161 difference between them regarding their underlying chemical mechanisms (Charrier and Anastasio,
162 2012). The quantifications were based on plate-reader spectrophotometry (Tecan Infinite M200 Pro,
163 Switzerland) in MilliQ water for AA, and in a phosphate buffer with a physiological pH value of 7.4 after



164 adding 5,5'-dithiobis(2-nitrobenzoic acid), with readings taken at different specified reaction times (Calas
165 et al., 2018; Borlaza et al., 2021b, 2022). The possible transition metal contamination of the buffer was
166 removed by Chelex 100 resin to reduce the background oxidation. The consumption rates of the AA or
167 DTT were obtained from the simple linear regression of the absorbance values in time at 265 and 412 nm,
168 respectively. The coefficients of determination R^2 for the regression were >0.90 when $<70\%$ of the initial
169 amount of the reagent was oxidised. Matrix absorbance was considered, and the quality assurance of the
170 determinations was performed by positive control tests (Borlaza et al., 2021b). The limits of detection
171 (LODs) for the AA and DTT assays were set at three times the standard deviation (SD) for the blank
172 extracts and were typically 0.008 and $0.0014 \text{ nmol min}^{-1}$, respectively. The experimental protocols were
173 described in more detail previously (Calas et al., 2017, 2018).

174

175 The OP data measured by the AA and DTT assays were normalised to $\text{PM}_{2.5}$ mass (m) or sampled air
176 volume (V) and are denoted as $\text{OP}_{\text{AA},m}$, $\text{OP}_{\text{DTT},m}$, $\text{OP}_{\text{AA},V}$ and $\text{OP}_{\text{DTT},V}$. The consumption rates normalized
177 to V are often considered to have a closer relationship to human exposure, while those normalized by m
178 are regarded as a measure of the inherent toxicity of PM (Weber et al., 2018; Yu et al., 2019).

179 **2.4 Mathematical models**

180 Source apportionment modelling was accomplished to identify and quantify the main aerosol sources
181 using positive matrix factorisation (PMF, US Environmental Protection Agency, version 5.0; EPA, 2017).
182 It decomposes the sample data matrix into a linear combination of two matrices: a daily factor contribution
183 varying in time and factor profiles by minimizing the critical compound parameter Q (Paatero and Tapper,
184 1994; Hopke, 2016, 2000). The input data set contained the concentrations and uncertainties of $\text{PM}_{2.5}$
185 mass, S, Cl, K, Ca, Ti, V, Cr, Mn, Fe, Ni, Cu, Zn, Br, Rb, Ba, Pb, EC, OC and LVG for all sampling sites
186 and seasons. A multisite PMF modelling with 143 samples was performed (Dai et al., 2020). For most
187 chemical species, all concentrations were higher than the LODs. For some trace elements, the
188 concentrations were larger than the LODs in $>60\%$ of the samples. The missing data were replaced by
189 the related median with an uncertainty of $5/6$ of the LOD value. The concentrations above LODs were
190 associated with an equation-based extra standard deviation in accordance with the guidelines of the PMF
191 manual, which involved the measurement uncertainty, the concentration and the LOD values (EPA,
192 2017). Elements Cl, Cr, Ni and Rb were specified as weak variables due to their relatively large SDs.

193

194 Several test runs were performed with a total number of factors ranging from 3 to 9 to define the base
195 runs. To explore the goodness of the individual results and to derive robust source apportionment,
196 additional mathematical tools such as bootstrapping and displacement methods were adopted (Norris et



197 al., 2014). In bootstrapping, the compliance between the base factors and bootstrapped factors (which
198 were later selected as the final solution) was >80 %. In addition, the displacement for these solutions did
199 not show larger changes in the parameter Q and no swap counts of factors occurred.

200

201 Multiple linear regression (MLR) modelling was performed to deconvolute the measured $OP_{AA,V}$ and
202 $OP_{DTT,V}$ data sets as the dependent variables among the main aerosol sources identified by the PMF as the
203 independent variables (Weber et al., 2021). A linear predictor function was fitted through the dependent
204 variable points by the weighted least squares (WLS) method. The weights were chosen as the inverse of
205 the square of the SD for each measured OP. Goodness of the fit was checked by residual analysis. The
206 significant predictor variables were selected using an F -test. The calculations were performed in the
207 advanced analytics software package Statistica (version 7.1, StatSoft, Germany).

208 **3 Results and discussion**

209 **3.1 Ranges, averages and tendencies**

210 Basic statistics of the daily OP data and atmospheric concentrations obtained from the filters for the whole
211 sampling interval in the three environments are summarised in Table 1. Some further atmospheric
212 concentrations measured online and the local meteorological data together with their measuring methods
213 are given in Sect. S1 in the Supplement. The concentrations of EC_{FF} , OC_{FF} , EC_{BB} , OC_{BB} , OC_{BIO} and SOC
214 derived earlier can be found in previous publications (Salma et al. 2020a, 2022). The present average
215 concentrations and meteorological data are in line with the results of earlier studies (Salma et al., 2004,
216 2005, 2020a; Szigei et al., 2015) suggesting that the overall data set represents typical atmospheric
217 conditions at the locations. However, several Saharan dust intrusions into the Carpathian Basin happened
218 in April 2018 (Varga, 2020). The most intensive event reached the region via southern Italy and the
219 Balkans on 15 April and affected the studied region for a few days.

220

221 The average $PM_{2.5}$ mass, OP_{AA} and OP_{DTT} data sets showed three different tendencies with respect to the
222 locations. This is better visualised with their annual mean and median data in Fig. 1. The averages (i.e.
223 the medians and means) of the $PM_{2.5}$ mass exhibited a rising trend with levelling off from the rural
224 background through the suburban area to the city centre. The means of both $OP_{AA,m}$ and $OP_{AA,V}$ data sets
225 indicated a maximum in the suburban background, whereas the tendencies for their medians were not
226 fully conclusive. The averages of both $OP_{DTT,m}$ and $OP_{DTT,V}$ data sets showed steadily increasing
227 behaviour. The differences in the tendencies already suggest that there is a misalignment between the PM



228 mass and the OP data and that the two assays used show different sensitivity to source types active at the
 229 locations.

230

231 **Table 1.** Ranges and medians of oxidative potential (OP) determined by AA and DTT assays and normalised to PM mass (m ;
 232 $OP_{AA,m}$ and $OP_{DTT,m}$, respectively, in unit of $\text{nmol min}^{-1} \mu\text{g}^{-1}$) or to sampled air volume (V ; $OP_{AA,V}$ and $OP_{DTT,V}$, respectively,
 233 $\text{nmol min}^{-1} \text{m}^{-3}$), of concentrations for $\text{PM}_{2.5}$ mass ($\mu\text{g m}^{-3}$), chemical elements (all in ng m^{-3}), elemental carbon (EC), organic
 234 carbon (OC, both in $\mu\text{g m}^{-3}$), levoglucosan (LVG, ng m^{-3}) in the rural background, suburban area and city centre.

235

Site/ Variable	Rural background			Suburban area			City centre		
	Minimum	Median	Maximum	Minimum	Median	Maximum	Minimum	Median	Maximum
$OP_{AA,m}$	0.01	0.12	0.28	0.02	0.14	0.33	0.03	0.11	0.23
$OP_{AA,V}$	0.1	1.5	5.2	0.3	2.4	11.7	0.3	2.1	4.9
$OP_{DTT,m}$	0.04	0.10	0.20	0.004	0.11	0.27	0.11	0.17	0.27
$OP_{DTT,V}$	0.3	1.2	3.1	0.03	1.9	6.2	1.3	2.9	6.1
$\text{PM}_{2.5}$	6	14	29	7	18	46	7	18	44
S	51	311	1043	84	312	823	167	367	952
Cl	5	11	28	5	32	118	5	23	71
K	11	56	234	9	65	363	18	91	264
Ca	1	33	215	6	73	457	23	104	468
Ti	0.05	1.3	15	0.3	1.9	26	0.6	3.1	22
V	0.23	0.46	1.1	0.13	0.43	1.0	0.13	0.44	1.2
Cr	0.16	0.37	0.91	0.18	0.46	1.7	0.17	0.76	7.2
Mn	0.4	2.0	16	0.1	2.1	5.6	0.5	3.3	11
Fe	5	32	162	16	63	306	33	102	607
Ni	0.13	0.42	1.3	0.14	0.33	1.1	0.18	0.57	3.0
Cu	0.13	0.94	6.8	0.6	1.6	7.5	0.8	2.9	27
Zn	0.9	7.2	40	3	12	53	1	17	48
Br	0.20	0.77	3.0	0.2	1.2	4.1	0.5	1.3	2.7
Rb	0.22	0.35	0.76	0.22	0.36	0.83	0.24	0.34	0.80
Ba	1.1	2.4	12	1.1	3.1	12	1.1	4.5	13
Pb	0.6	3.4	28	1.5	5.3	21	1.3	5.6	19
EC	0.08	0.22	0.77	0.21	0.50	1.1	0.31	0.78	1.8
OC	0.9	2.3	6.0	1.0	2.9	11	2.0	3.3	8.0
LVG	4	38	776	5	106	1765	8	203	709

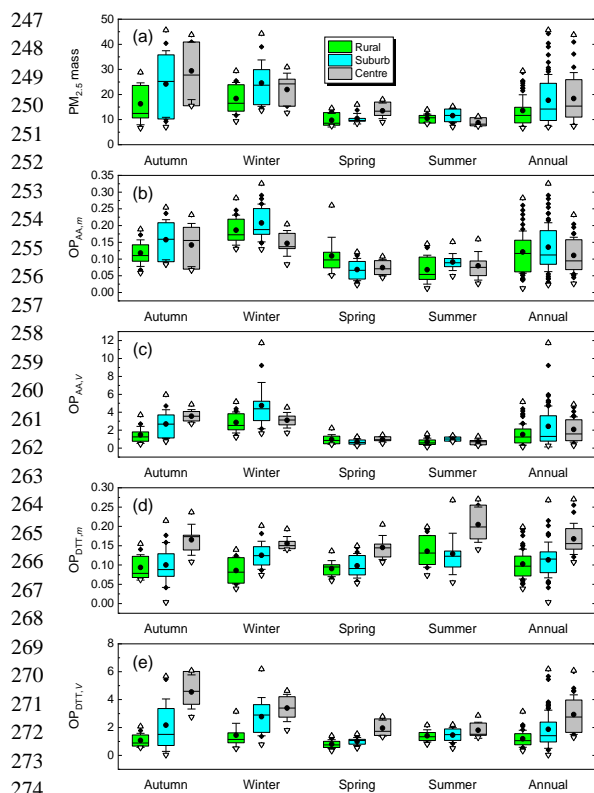
236

237 Basic statistics of $\text{PM}_{2.5}$ mass and OP data separately for each season and the whole year are shown in
 238 Fig. 1. In winter and autumn (the heating period), the OP and PM mass levels were higher than in spring
 239 and summer. This is consistent with the other continental European sites (e.g. Calas et al., 2019; Borlaza
 240 et al., 2022). The heating period-to-non-heating period OP ratios in the urban locations were larger than
 241 for the rural background by factors of ca. 4 for $OP_{AA,V}$ and 1–2 for $OP_{DTT,V}$. There were similar tendencies
 242 in the OP values derived by both AA and DTT assays over the seasons. Except for the $OP_{DTT,m}$ data,
 243 which showed a fairly constant level over the seasons with some higher values in summer, particularly in



244 the city centre. This can be again linked to the altered chemical composition of PM mass in time and to
 245 the different responses of the two assays to this change.

246



275 **Figure 1.** Box and whisker plots of PM_{2.5} mass concentration ($\mu\text{g m}^{-3}$; panel a), oxidative potential (OP) determined by AA
 276 and DTT assays and normalised to PM mass (m ; $\text{OP}_{\text{AA},m}$ and $\text{OP}_{\text{DTT},m}$, $\text{nmol min}^{-1} \mu\text{g}^{-1}$; panels b and d) or to sampled air
 277 volume (V ; $\text{OP}_{\text{AA},V}$ and $\text{OP}_{\text{DTT},V}$, $\text{nmol min}^{-1} \text{m}^{-3}$; panels c and e) in the rural background, suburban area and city centre
 278 separately for each season and over one year. Maximum and minimum values (triangles pointing upward and downward,
 279 respectively), further extreme values (diamonds), the first and third quartiles (lower and upper horizontal borders of the boxes,
 280 respectively), median (horizontal line inside the boxes), means (bullets) and ± 1 SDs (whiskers) of the data sets are shown.

281

282 There are only a few other OP data sets for the PM_{2.5} size fraction derived by AA and DTT assays. Their
 283 comparison to our OP data is hindered by important experimental details such as the extracted amount of
 284 PM from filters. It can be roughly identified that our median OP values are somewhat larger than those at
 285 other European sites (Daellenbach et al., 2020; Grange et al., 2022, In 't Veld et al., 2023), while they
 286 belong to the middle range of the available results for Japan and China (Kurihara et al., 2022; Yu et al.,

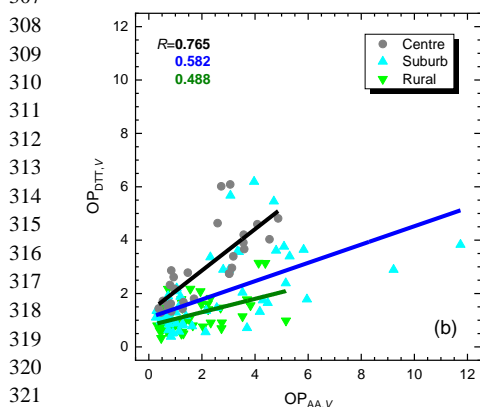
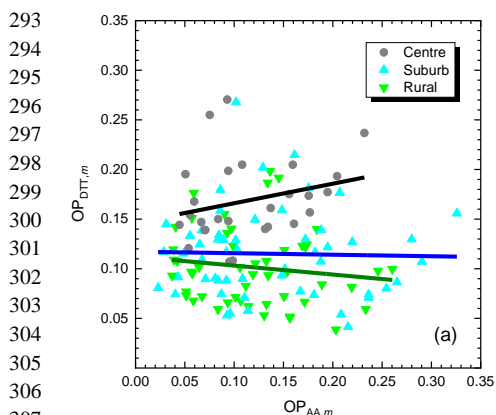


287 2019). The differences can be also influenced by the exact location type since higher OP data near traffic
 288 sources were observed (Boogaard et al., 2012; Fang et al., 2016; Daellenbach et al., 2020).

289 3.2 Consistency between the assays

290 The dependencies between the OP data derived by the AA assay and normalised either to m or V on the
 291 corresponding DTT data are displayed in Fig. 2.

292



323 **Figure 2.** Scatter plots of the oxidative potential (OP) values determined by AA and DTT assays and normalised to PM mass
 324 (m ; $OP_{AA,m}$ and $OP_{DTT,m}$, in $\text{nmol min}^{-1} \mu\text{g}^{-1}$; panel a) or to sampled air volume (V ; $OP_{AA,V}$ and $OP_{DTT,V}$, $\text{nmol min}^{-1} \text{m}^{-3}$; panel
 325 b) separately in the rural background, suburban area and city centre. The coefficients of correlation (R s) for the significant
 326 cases are also given.

327

328 Pearson's coefficients of correlation (R) between the data sets normalised to m (Fig. 2a) were not
 329 significant ($p=0.05$) at the locations. It suggests that the OP_m was controlled by chemical species that
 330 invoked different responses in the assays. However, all correlations between the two OP data sets



331 normalised to V (Fig. 2b) were significant. The slopes with SDs of the regression lines were smaller than
332 unity (0.25 ± 0.06 , 0.34 ± 0.07 and 0.78 ± 0.13 , respectively) and increased monotonically from the rural
333 background through the suburban area to the city centre.

334

335 The results suggested that the OP values normalised to sampled air volume were coherent. The AA assay
336 reacted more sensitively to the changes in chemical composition of PM than the DTT assay at our
337 locations. The increasing slope of the regression could be also connected to the fact that organics of
338 biogenic origin exhibit smaller responses in the DTT assays than those of BB (Verma et al., 2015) or of
339 urban sources in general. The differences could be partly influenced by aerosol photochemical aging and
340 SOC formation over seasons (Wong et al., 2019; Zhang et al., 2022). More importantly, the conclusions
341 definitely underline the need for deploying multiple (at least two) OP assays, particularly in cleaner
342 atmospheric environments, to achieve a more holistic and consistent picture (Bates et al., 2019; Calas
343 et al., 2017; Borlaza et al., 2022).

344 3.3 Main aerosol sources

345 Six factors resolved by the PMF modelling were further evaluated as described in Sect. S2. The following
346 aerosol sources were identified: biomass burning, suspended dust, road traffic, oil combustion, vehicle
347 metal wear and mixed industrial source. Similar set of source types was also identified earlier for Budapest
348 in larger number of samples in winter (Furu et al., 2022).

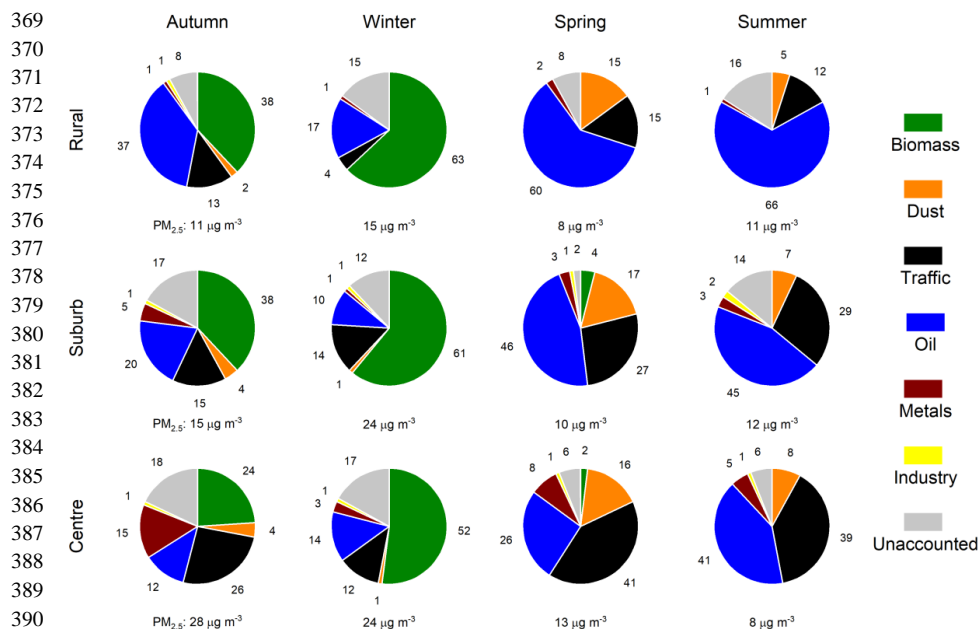
349

350 The apportionments of the $PM_{2.5}$ mass among the main sources are summarised in Fig. 3 separately for
351 each location and season. The plots reveal that the source contributions changed very substantially over
352 the year. In winter, BB was the dominant source (with mean contributions of 50 % – 60 %) at all sites. In
353 autumn, BB and oil combustion were the two most important sources in the rural background with similar
354 shares (38 %). In the suburban area, BB exhibited very similar (38 %) contribution to the rural
355 background, whereas oil combustion and the joint importance of road traffic and vehicle metal wear
356 showed the second largest and similar contributions (20 %). In the city centre, traffic-related sources were
357 the most important contributors (40 %). In spring, oil combustion prevailed (60 %) in the rural
358 background. Its contribution monotonically decreased through the suburban area (46 %) to the city centre
359 (26 %). In parallel with this tendency, the joint share from road traffic and vehicle metal wear increased
360 monotonically (from 17 % through 30 % to 49 %) in the same order of the locations. The contributions
361 from suspended dust in spring were also significant at all locations accounting for approximately 15%.
362 They were influenced by the Saharan dust intrusion episodes extending over the whole Carpathian Basin
363 in this season. In summer, oil combustion was again the dominant source (66 %) in the rural background



364 and showed a decreasing share for the suburban area (45 %) to the city centre (41 %). Contrary, the effects
 365 of road traffic monotonically rose (from 13 % through 31 % to 44 %). This increasing tendency was
 366 preserved in the other seasons as well. The unaccounted sources and their possible effects on the final
 367 results are discussed in Sect. 3.6.

368



392 **Figure 3.** Mean contributions of biomass burning, suspended dust, road traffic, oil combustion, vehicle metal wear, mixed
 393 industrial source and unaccounted sources to the atmospheric concentration of PM_{2.5} mass (in %) as derived by the PMF
 394 modelling in the rural background, suburban area and city centre in different seasons. The median atmospheric concentrations
 395 are shown under the circle charts.

396

397 The apportionments of Cu and Fe, which are of special interest for OP, among the main aerosol sources
 398 as derived by the PMF modelling are shown in Figs. S7 and S8. Copper mainly or dominantly originated
 399 from motor vehicles, i.e. vehicle metal wear and road traffic sources except for the rural background in
 400 winter and autumn. The outstanding role of road vehicles is confirmed by our earlier results for a street
 401 canyon in central Budapest (Salma and Maenhaut, 2006). The smallest shares from vehicles occurred in
 402 winter (22 %, 39 % and 65 %, respectively in the rural background, suburban area and city centre), while
 403 the maximum contributions happened in summer (51 %, 65 % and 87 %, respectively). The contribution
 404 of unaccounted sources in the rural background in winter was large (33 %), which could modify the
 405 apportionments. The role of BB in Cu emissions could be possible explained by illegal industrial and
 406 household waste burnings together with biomass (Sect. S2; Hoffer et al., 2021).



407

408 In the city centre, the vehicle sources showed the largest contributions to Fe (53 % – 74 %) in all seasons,
409 and dust was its second most intensive source (30 %–36 %) in spring and summer. At the other two
410 locations, Fe in spring was unambiguously dominated by dust (ca. 55 %), which was influenced by the
411 Saharan dust intrusion. Suspended dust remained the most important source in the rural background in
412 summer, whereas it became comparable to the traffic-related sources in the suburban area. Vehicles
413 tended to be the second largest Fe source (26 % – 45 %) in the rural background and suburban area. Their
414 contributions could be partly also associated with the resuspended road dust generated by moving
415 vehicles. In autumn, the shares in the rural background were more or less balanced among the main
416 sources, while the vehicle contributions were increased in the suburban area.

417

418 The examples of Cu and Fe demonstrated broadly varying spatial and temporal tendencies in the source
419 contributions of OP-active chemical species, and point to the potentials of regulatory measures based on
420 specifically selected source types.

421 **3.4 Oxidative potential and aerosol sources**

422 The OP data normalised to sampled air volume were apportioned to the main aerosol sources, i.e. of BB,
423 suspended dust, road traffic, oil combustion, vehicle metal wear and mixed industrial source using the
424 MLR method with the WLS approach. The slopes and intersects of the regression lines calculated for the
425 whole data set at each sampling location are summarised in Table S4. In a few cases, negative slopes were
426 obtained. This is commonly found with this approach, but the absolute values of the negative slopes
427 should be relatively small. This was not the case for the vehicle metal wear and $OP_{DTT,V}$ pair in the rural
428 background, for the road traffic and $OP_{AA,V}$ pair in the suburban area, and for the oil combustion and
429 $OP_{AA,V}$ pair in the city centre. The intersects of the $OP_{DTT,V}$ in the suburban area and city centre also
430 resulted in statistically nonzero values. These cases jointly indicate that there could be some aerosol
431 sources missing in the PMF modelling due probably to the unavailability of some important marker
432 variables and to the limited number of samples. The shortcoming is further discussed in Sect. 3.6. It cannot
433 be excluded that this imperfection influences the order and mainly the contributions of the OP sources.
434 To improve the attribution of the OP to the identified aerosol sources, the MLR model with the WLS
435 approach was also performed with forced positive slopes option. Its constrained results are summarised
436 in Table 2.

437

438 With this latter option, all intersects became statistically insignificant ($p < 0.05$) from zero. The AA assay
439 yielded significant slopes with BB, road traffic and oil combustion in the rural background, with BB and



440 suspended dust in the suburban area and with BB, and road traffic in the city centre. The DTT assay
 441 resulted in significant slopes with BB and road traffic, with BB and oil combustions and with BB and
 442 road traffic in the three environments. Comparing the fitted MLR parameters obtained by the constrained
 443 and non-constrained WLS approaches (Tables 2 and S4) shows that the orders of the sources did not
 444 change substantially, and that the positive slopes obtained by the two models are comparable. At the same
 445 time, the importance of oil combustion decreased in some occasions. These likely indicate that the derived
 446 ranks of the OP sources are sensible approximations to reality with some larger uncertainties of their
 447 contributions.

448

449 **Table 2.** Slopes and intersects of the multiple linear regression with the weighted least squares approach and forced positive
 450 slopes option between oxidative potential (OP) determined by AA and DTT assays and normalised to sampled air volume
 451 ($OP_{AA,V}$ and $OP_{DTT,V}$, respectively) and the main aerosol sources of biomass burning, suspended dust, road traffic, oil
 452 combustion, vehicle metal wear and mixed industrial source derived by PMF modelling in the rural background, suburban area
 453 and city centre. The number of samples available (n) and the adjusted coefficients of determination (R^2) are also shown.
 454 Nonsignificant values are in *Italic* font.

455

Location/ Main source	Rural background		Suburban area		City centre	
	$OP_{AA,V}$	$OP_{DTT,V}$	$OP_{AA,V}$	$OP_{DTT,V}$	$OP_{AA,V}$	$OP_{DTT,V}$
Biomass burning	1.414	0.873	0.792	0.622	1.073	0.788
Suspended dust	<i>0.113</i>	–	0.569	<i>0.018</i>	<i>0.025</i>	<i>0.090</i>
Road traffic	1.010	0.959	–	<i>0.181</i>	0.357	0.887
Oil combustion	0.279	–	<i>0.522</i>	0.968	–	<i>0.488</i>
Vehicle metal wear	<i>0.056</i>	–	–	–	<i>0.018</i>	<i>0.091</i>
Mixed industrial	–	<i>0.085</i>	<i>0.172</i>	<i>0.086</i>	<i>0.142</i>	–
Intersect	<i>-0.160</i>	<i>0.358</i>	<i>-0.473</i>	<i>-0.497</i>	<i>-0.081</i>	<i>-0.362</i>
N	52	51	56	55	28	28
R^2	0.974	0.877	0.717	0.779	0.858	0.811

456

457 The driving effect of BB on OP has been highlighted in other studies (e.g. Verma et al., 2015; Lionetto et
 458 al., 2021; Borlaza et al., 2022). The intensity of BB in the Carpathian Basin is, however, large only in the
 459 heating period (autumn and winter), and much lower outside this interval. To refine the apportionment of
 460 the OP data to aerosol sources active in the non-heating seasons, the MLR modelling was repeated with
 461 the joint data set of all sites split into heating and non-heating periods. These results confirmed that BB
 462 shows overwhelming contributions to the OP values in the heating period. More importantly, the obtained
 463 results also imply that the shares from vehicles (i.e. joint sources of road traffic and vehicle metal wear)
 464 in the non-heating period to OP prevailed. This is in line with the attributions of some transition metals



465 such as Cu and Fe to these aerosol sources (Figs. S7–S8 and Salma and Maenhaut, 2006), and also points
466 to the remarkable role of primary traffic emissions in causing oxidative stress in spring and summer.

467

468 Secondary organic aerosol under anthropogenically influenced conditions was proven to be one of the top
469 factors for OP (Srivastava et al., 2018; Wong et al., 2019; Daellenbach et al., 2020; Borlaza et al., 2021a,
470 2021b; Pye et al., 2021; Zhang et al., 2022). The involvement of the SOC concentrations into the PMF
471 was hampered by their smaller count and larger relative uncertainty (up to 30 % – 50 %; Salma et al.,
472 2022). Instead, we investigated the correlations between the OP data sets and SOC concentrations or
473 SOC/OC ratios. The dependencies of the $OP_{DTT,V}$ on the SOC are shown in Fig. S9. The OP values at the
474 urban locations tended to increase with the SOC in parallel with each other, while the OP was rising in a
475 smaller rate in the regional background. The reasons behind these observations likely include the distinct
476 effects of biogenic and anthropogenic secondary organic aerosols typically present in different portions
477 at the sampling locations. The results may also indirectly indicate that photochemical aging processes
478 impact the toxicity of PM as well (Kodros et al., 2020). There were no significant correlations obtained
479 for the other data pairs.

480 **3.5 Oxidative potential and air quality**

481 Particulate matter mass was proven to be the most important proximity metric from the criteria air
482 pollutants for the general air quality in the Carpathian Basin (Salma et al., 2020a, 2020b). Therefore, the
483 relationships between the $PM_{2.5}$ mass and OP data sets normalised to sampled air volume were separately
484 investigated. Their correlation dependencies were all significant (Fig. 4). Spatial and temporal
485 correlations between these variables from low to moderate were also observed in earlier studies under
486 broadly varying conditions (Künzli et al., 2006; Boogaard et al., 2012; Yang et al., 2015; Fang et al.,
487 2016; Chirizzi et al., 2017).

488

489 The dependencies for the $OP_{DTT,V}$ (Fig. 4a) resulted in two almost parallel lines (with slopes and SDs of
490 0.11 ± 0.01 and 0.13 ± 0.01 $\text{nmol min}^{-1} \mu\text{g}^{-1}$, respectively) in the city centre and suburban area, while a
491 smaller slope (0.051 ± 0.012 $\text{nmol min}^{-1} \mu\text{g}^{-1}$) was observed in the rural background. The situation for the
492 $OP_{AA,V}$ (Fig. 4b) was less obvious but somewhat similar to $OP_{DTT,V}$. The regression lines for the rural
493 background and suburban area tended to be fairly parallel with each other (with slopes and SDs of
494 0.16 ± 0.02 and 0.18 ± 0.02 $\text{nmol min}^{-1} \mu\text{g}^{-1}$, respectively), whereas the slope for the city centre was smaller
495 (0.096 ± 0.019 $\text{nmol min}^{-1} \mu\text{g}^{-1}$). The intersects could be typically regarded to be zero within the
496 uncertainty interval.



497

498 The parallel tendencies may indicate that the effects of the PM chemical compositions on the given assay
 499 were close to each other at the sampling locations with the parallel lines. This was likely caused by spatial
 500 and temporal similarities in the main sources such as road traffic and resuspended dust particularly for
 501 the DTT assay, and biomass burning especially for the AA assay (Salma et al., 2020a). Particles in the
 502 third environment (with the smaller slope) likely contained less OP-active components from the point of
 503 the given assay and, therefore, the increase in the OP was more modest. This interpretation is confirmed
 504 by earlier similar conclusions (Daellenbach et al., 2020). Nevertheless, it should be stressed that all slopes
 505 were substantially and much smaller than unity. This implies that the air quality regulatory measures
 506 based on the $PM_{2.5}$ mass are expected to result in smaller improvements in oxidative stress compared to
 507 dedicated measures that specifically target (appropriately selected) aerosol sources.

508

509

510

511

512

513

514

515

516

517

518

519

520

521

522

523

524

525

526

527

528

529

530

531

532

533

534

535

536

537

538

539

540

541

542

543

544

545

546

547

548

549

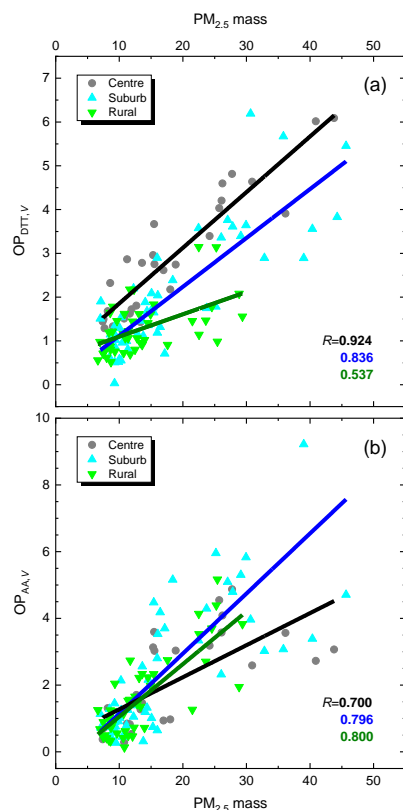


Figure 4. Scatter plots of the oxidative potential (OP) determined by DTT (a) and AA (b) assays and normalised to sampled
 air volume (V ; $OP_{DTT,V}$ and $OP_{AA,V}$, respectively, in $nmol\ min^{-1}\ m^{-3}$) and $PM_{2.5}$ mass concentrations ($\mu g\ m^{-3}$) for the rural
 background, suburban area and city centre. The lines represent linear regressions of the data sets. The coefficients of correlation
 (R_s) are also indicated.



542 **3.6 Limitations and later possibilities**

543 The total numbers of the samples collected at each location represent a limitation mainly for the PMF
544 modelling. To overcome this problem, we applied multisite PMF. It was implicitly assumed in this
545 approach that the main sources active at the locations can be characterised by similar chemical profiles.
546 This is not completely fulfilled for all seasons. An example is the suspended dust which is virtually
547 fugitive mineral and soil dust made of geogenic elements in the rural backgrounds. In the urban sites, it
548 contains further constituents originally generated by anthropogenic activities, which settled down to
549 surfaces and later entered into the air again by resuspension. It is mentioned that the PMF modelling on
550 the separate locations yielded fairly similar results to the multisite approach, while the statistical
551 uncertainties of these latter calculations were favourable.

552

553 The unavailability of some secondary inorganics, mainly nitrate and ammonium ions in the present
554 analytical data sets introduced another limitation. Their contributions were likely contained in the
555 unaccounted sources of the PMF modelling. They ranged up to 18 % and showed contributions mainly in
556 colder (heating) seasons or in summer for the rural background and suburban area. Fortunately, pure
557 secondary inorganic constituents are associated with lower contribution to PM toxicity (Cassee et al.,
558 2013; Daellenbach et al., 2020), although they can influence the OP through acid mediated dissolution of
559 transition metals (Fang et al., 2017). However, the robustness of the PMF modelling can influence the
560 final apportionment of the OP among the resolved sources.

561

562 Larger number of samples and extended list of variables are pronouncedly required because of the basin
563 character of the region of interest. The poorest air quality in the whole Carpathian Basin generally occurs
564 in winter (Salma et al., 2022), when persistent anticyclonic weather situations and lasting temperature
565 inversions happen for longer times. During these intervals, the time series of aerosol constituents, even
566 of different origins, change coherently at many locations due to the common effects of regional
567 meteorology. This dependency can further encumber the separation of the aerosol sources in PMF
568 modelling (Salma et al., 2004).

569

570 The present results and conclusions can be further improved by involving additional important chemical
571 species and markers, mainly water-soluble metal ions, water-soluble OC, primary biogenic OC and PAHs.
572 Extended research is required to address some additional relevant sources such as coal combustion,
573 biogenic emissions and illegal waste burning. Investigations of size-fractionated aerosol samples with
574 several toxicity indicators including intracellular tests and possible synergism or antagonism among



575 chemical species could bring further insights into the oxidative stress research. The experience gained in
576 the present work, which was conducted in a systematic manner for the first time in this region, can form
577 valuable experience in planning further related studies.

578 **4 Conclusions**

579 We showed that the OP induced by PM_{2.5} mass and determined by the AA and DTT assays in the rural
580 (regional) background of the Carpathian Basin, in the suburban area and centre of its largest city of
581 Budapest differed substantially and in a complex manner with location and changed considerably and
582 consistently with season. The alterations were mainly caused by varying intensities of the main aerosol
583 sources and possibly by other specific seasonal features. Biomass burning clearly exhibited the dominant
584 influence at all locations in the heating period. Several pieces of indirect evidence suggest that the joint
585 effects of motor vehicles involving road traffic and vehicle metal wear played the most important role in
586 summer and spring, with considerable contributions from oil combustion and resuspended dust.

587

588 The most severe daily PM health limit exceedances in Budapest (and several other European cities) occur
589 in winter due to both residential heating and meteorological effects. The contributions of BB to OP are
590 the largest during this season. Thus, human exposure to high pollution levels are further exacerbated by
591 the chemical composition which causes increased oxidative stress. As far as the sources related to motor
592 vehicles are concerned, large traffic intensities frequently occur in city centres, which generate dangerous
593 hotspots of particularly OP-active species. In these sites, an enhanced exposure of public in summer and
594 spring often coincides with high population densities.

595

596 Our conclusions imply that targeting the PM mass in general does not efficiently reduce the oxidative
597 burden from PM exposure. Instead, substantial health improvements could be achieved by focusing on
598 some specific source types such as BB in winter and vehicle traffic in non-heating period. The former
599 source may have timely consequences since it is expected to be increased in the near future. The non-
600 exhaust emissions from vehicle traffic are anticipated to gain in relevance as well since high-efficiency
601 exhaust gas aftertreatment devices had been already adopted to internal combustion engines and because
602 of global spreading of electric vehicles. The advantages of BB and electric cars are often emphasized,
603 while their potential drawbacks have been less disseminated. It is needed to further investigate their
604 distinctive health effects for setting up effective mitigation policies and season-specific regulations.

605 *Data availability.* The observational data are available from the corresponding author.

606 *Supplement.* The supplement related to this article is available online at: *to be completed.*



607 *Author contributions.* MV evaluated the data, performed the modelling calculations, prepared figures, participated in
608 interpreting the results and contributed to writing the manuscript; GU and J-LJ managed the OP measurements, GU, J-LJ
609 PD participated in interpreting the results and revising the manuscript; ZsK and EP managed the PIXE measurements and
610 participated in interpreting the PMF results; IS conceived the research, arranged the sample collections, evaluated and
611 interpreted the results, prepared figures, wrote the manuscript. All coauthors reviewed and commented on the manuscript.

612 *Competing interests.* The authors declare that they have no conflict of interest.

613 *Acknowledgements.* The authors are grateful to Anikó Angyal of the Institute for Nuclear Research for the PIXE measurements,
614 to Attila Machon of the Hungarian Meteorological Service for the assistance in the sample collections and the OC/EC
615 measurements, and to Anikó Vasanits of the Eötvös Loránd University for the LVG measurements.

616 *Financial support.* This research has been supported by the Hungarian Research, Development and Innovation Office (grants
617 K132254 and K146915), the European Regional Development Fund and the Hungarian Government (grant GINOP-2.3.3-15-
618 2016-00005) and the New National Excellence Program of the Ministry for Innovation and Technology from the source of the
619 Hungarian Research, Development and Innovation Fund (ÚNKP-21-3). The OP analysis was supported by the ACME program
620 (ANR-15-IDEX-02) and ANR Get OP Stand OP program (ANR-19-CE34-0002-01), and were analyzed at the Air-O-Sol
621 facility at IGE, made possible with the funding of some laboratory equipment by the Labex OSUG@2020 (ANR10 LABX56).

622 **References**

- 623 Abrams, J. Y., Weber, R. J., Klein, M., Samat, S. E., Chang, H. H., Strickland, M. J., Verma, V., Fang, T., Bates, J. T.,
624 Mulholland, J. A., Russell, A. G., and Tolbert, P. E.: Associations between ambient fine particulate oxidative potential
625 and cardiorespiratory emergency department visits, *Environ. Health Perspect.*, 125, 107008,
626 <https://doi.org/10.1289/EHP1545>, 2017.
- 627 Aljboor, S., Angyal, A., Baranyai, D., Kertész, Zs., Papp, E., Szarka, M., Szikszai, Z., Rajta, I., and Vajda, I.: Light element
628 sensitive in-air millibeam-PIXE setup for fast measurement of atmospheric aerosol samples, *J. Anal. At. Spectrom.*,
629 submitted in 2022.
- 630 Apte, J. S., Marshall, J. D., Cohen, A. J., and Brauer, M.: Addressing global mortality from ambient PM_{2.5}, *Environ. Sci.*
631 *Technol.*, 49, 8057–8066, <https://doi.org/10.1021/acs.est.5b01236>, 2015.
- 632 Ayres, J. G., Borm, P., Cassee, F. R., Castranova, V., Donaldson, K., Ghio, A., Harrison, R. M., Hider, R., Kelly, F., Kooter,
633 I. M., Marano, F., Maynard, R. L., Mudway, I., Nel, A., Sioutas, C., Smith, S., Baeza-Squiban, A., Cho, A., Duggan, S.,
634 and Froines, J.: Evaluating the toxicity of airborne particulate matter and nanoparticles by measuring oxidative stress
635 potential– a workshop report and consensus statement, *Inhal. Toxicol.* 20, 75–99,
636 <https://doi.org/10.1080/08958370701665517>, 2008.
- 637 Baumann, K., Wietzoreck, M., Shahpoury, P., Filippi, A., Hildmann, S., Lelieveld, S., Berkemeier, T., Tong, H., and
638 Lammel, G.: Is the oxidative potential of components of fine particulate matter surface-mediated?, *Environ. Sci. Pollut.*
639 *Res.*, 30, 16749–16755, <https://doi.org/10.1007/s11356-022-24897-3>, 2023.
- 640 Bates, J. T., Weber, R. J., Abrams, J., Verma, V., Fang, T., Klein, M., Strickland, M. J., Sarnat, S. E., Chang, H. H.,
641 Mulholland, J. A., Tolbert, P. E., and Russell, A. G.: Reactive oxygen species generation linked to sources of
642 atmospheric particulate matter and cardiorespiratory effects, *Environ. Sci. Technol.*, 49, 13605–13612,
643 <https://doi.org/10.1021/acs.est.5b02967>, 2015.
- 644 Bates, J. T., Fang, T., Verma, V., Zeng, L., Weber, R. J., Tolbert, P. E., Abrams, J. Y., Sarnat, S. E., Klein, M., Mulholland,
645 J. A., and Russell, A. G.: Review of acellular assays of ambient particulate matter oxidative potential: methods and
646 relationships with composition, sources, and health effects, *Environ. Sci. Technol.*, 53, 4003–4019,
647 <https://doi.org/10.1021/acs.est.8b03430>, 2019.
- 648 Blumberger, Z. I., Vasanits-Zsigrai, A., Farkas, G., and Salma, I.: Mass size distribution of major monosaccharide
649 anhydrides and mass contribution of biomass burning, <https://doi.org/10.1016/j.atmosres.2019.01.001>, *Atmos. Res.*,
650 220, 1–9, 2019.
- 651 Boogaard, H., Janssen, N. A. H., Fischer, P. H., Kos, G. P. A., Weijers, E. P., Cassee, F. R., van der Zee, S. C., de Hartog, J.
652 J., Brunekreef, B., and Hoek G.: Contrasts in oxidative potential and other particulate matter characteristics collected
653 near major streets and background locations, *Environ. Health Perspect.*, 120, 2, <https://doi.org/10.1289/ehp.1103667>,
654 2012.
- 655 Bondy, S. C.: Anthropogenic pollutants may increase the incidence of neurodegenerative disease in an aging population,
656 *Toxicology*, 341–343, 41–46, <https://doi.org/10.1016/j.tox.2016.01.007>, 2016.



- 657 Borlaza, L. J. S., Weber, S., Uzu, G., Jacob, V., Cañete, T., Micallef, S., Trébuchon, C., Slama, R., Favez, O., and Jaffrezo,
658 J.-L.: Disparities in particulate matter (PM₁₀) origins and oxidative potential at a city scale (Grenoble, France) – Part 1:
659 Source apportionment at three neighbouring sites, *Atmos. Chem. Phys.*, 21, 5415–5437, [https://doi.org/10.5194/acp-21-](https://doi.org/10.5194/acp-21-5415-2021)
660 5415-2021, 2021a.
- 661 Borlaza, L. J. S., Weber, S., Jaffrezo, J.-L., Houdier, S., Slama, R., Rieux, C., Albinet, A., Micallef, S., Trébuchon, C., and
662 Uzu, G.: Disparities in particulate matter (PM₁₀) origins and oxidative potential at a city scale (Grenoble, France) – Part
663 2: Sources of PM₁₀ oxidative potential using multiple linear regression analysis and the predictive applicability of
664 multilayer perceptron neural network analysis, *Atmos. Chem. Phys.*, 21, 9719–9739, [https://doi.org/10.5194/acp-21-](https://doi.org/10.5194/acp-21-9719-2021)
665 9719-2021, 2021b.
- 666 Borlaza, L. J., Weber, S., Marsal, A., Uzu, G., Jacob, V., Besombes, J.-L., Chatain, M., Conil, S., and Jaffrezo, J.-L.: Nine-
667 year trends of PM₁₀ sources and oxidative potential in a rural background site in France, *Atmos. Chem. Phys.*, 22,
668 8701–8723, <https://doi.org/10.5194/acp-22-8701-2022>, 2022.
- 669 Borm, P. J. A., Kelly, F., Künzli, N., Schins, R. P. F., and Donaldson, K.: Oxidant generation by particulate matter: from
670 biologically effective dose to a promising, novel metric, *Occup. Environ. Med.*, 64, 73–74,
671 <https://doi.org/10.1136/oem.2006.029090>, 2007.
- 672 Calas, A., Uzu, G., Martins, J. M. F., Voisin, D., Spadini, L., Lacroix, T., and Jaffrezo, J.-L.: The importance of simulated
673 lung fluid (SLF) extractions for a more relevant evaluation of the oxidative potential of particulate matter, *Sci. Rep.* 7,
674 11617, <https://doi.org/10.1038/s41598-017-11979-3>, 2017.
- 675 Calas, A., Uzu, G., Kelly, F. J., Houdier, S., Martins, J. M. F., Thomas, F., Molton, F., Charron, A., Dunster, C., Oliete, A.,
676 Jacob, V., Besombes, J.-L., Chevrier, F., and Jaffrezo, J.-L.: Comparison between five acellular oxidative potential
677 measurement assays performed with detailed chemistry on PM₁₀ samples from the city of Chamonix (France), *Atmos.*
678 *Chem. Phys.*, 18, 7863–7875, <https://doi.org/10.5194/acp-18-7863-2018>, 2018.
- 679 Calas, A., Uzu, G., Besombes, J.-L., Martins, J. M. F., Redaelli, M., Weber, S., Charron, A., Albinet, A., Chevrier, F.,
680 Brulfert, G., Mesbah, B., Favez, O., and Jaffrezo, J.-L.: Seasonal variations and chemical predictors of oxidative
681 potential (OP) of particulate matter (PM), for seven urban French sites, *Atmosphere*, 10, 698,
682 <https://doi.org/10.3390/atmos10110698>, 2019.
- 683 Cassee, F. R., Héroux, M.-E., Gerlofs-Nijland, M. E., and Kelly, F. J.: Particulate matter beyond mass: recent health
684 evidence on the role of fractions, chemical constituents and sources of emission, *Inhal. Toxicol.*, 25, 802–812,
685 <https://doi.org/10.3109/08958378.2013.850127>, 2013.
- 686 Cavalli, F., Viana, M., Yttri, K. E., Genberg, J., and Putaud, J.-P.: Toward a standardised thermal-optical protocol for
687 measuring atmospheric organic and elemental carbon: the EUSAAR protocol, *Atmos. Meas. Tech.*, 3, 79–89,
688 <https://doi.org/10.5194/amt-3-79-2010>, 2010.
- 689 Charrier, J. G. and Anastasio, C.: On dithiothreitol (DTT) as a measure of oxidative potential for ambient particles: evidence
690 for the importance of soluble transition metals, *Atmos. Chem. Phys.*, 12, 9321–9333, [https://doi.org/10.5194/acp-12-](https://doi.org/10.5194/acp-12-9321-2012)
691 9321-2012, 2012.
- 692 Charrier, J. G., McFall, A. S., Vu, K. K.-T., Baroi, J., Olea, C., Hasson, A., and Anastasio, C.: A Bias in the “Mass-
693 Normalized” DTT Response – An Effect of Non-Linear Concentration-Response Curves for Copper and Manganese,
694 *Atmos. Environ.*, 144, 325–334, <https://doi.org/10.1016/j.atmosenv.2016.08.071>, 2016.
- 695 Chiari, M., Yubero, E., Calzolari, G., Lucarelli, F., Crespo, J., Galindo, N., Nicolás, J. F., Giannoni, M., and Nava, S.:
696 Comparison of PIXE and XRF analysis of airborne particulate matter samples collected on Teflon and quartz fibre
697 filters, *Nucl. Instrum. Meth. B*, 417, 128–132, <https://doi.org/10.1016/j.nimb.2017.07.031>, 2018.
- 698 Chirizzi, D., Cesari, D., Guascito, M. R., Dinoi, A., Giotta, L., Donato, A., and Contini, D.: Influence of Saharan dust
699 outbreaks and carbon content on oxidative potential of water-soluble fractions of PM_{2.5} and PM₁₀, *Atmos. Environ.*,
700 163, 1–8, <https://doi.org/10.1016/j.atmosenv.2017.05.021>, 2017.
- 701 Cho, A. K., Sioutas, C., Miguel, A. H., Kumagai, Y., Schmitz, D. A., Singh, M., Eiguren-Fernandez, A., and Froines, J. R.:
702 Redox activity of airborne particulate matter at different sites in the Los Angeles Basin, *Environ. Res.*, 99, 40–47,
703 <https://doi.org/10.1016/j.envres.2005.01.003>, 2005.
- 704 Cohen, A., Brauer, M., Burnett, R., Anderson, H., Frostad, J., Estep, K., Balakrishnan, K., Brunekreef, B., Dandona, L.,
705 Dandona, R., Feigin, V., Freedman, G., Hubbell, B., Jobling, A., Kan, H., Knibbs, L., Liu, Y., Martin, R., Morawska,
706 L., and Forouzanfar, M.: Estimates and 25-year trends of the global burden of disease attributable to ambient air
707 pollution: An analysis of data from the Global Burden of Diseases Study 2015, *The Lancet*, 389, 1907–1918,
708 [https://doi.org/10.1016/S0140-6736\(17\)30505-6](https://doi.org/10.1016/S0140-6736(17)30505-6), 2017.
- 709 Daellenbach, K. R., Uzu, G., Jiang, J., Cassagnes, L.-E., Leni, Z., Vlachou, A., Stefenelli, G., Canonaco, F., Weber, S.,
710 Segers, A., Kuenen, J. J. P., Schaap, M., Favez, O., Albinet, A., Aksoyoglu, S., Dommen, J., Baltensperger, U., Geiser,



- 711 M., El Haddad, I., Jaffrezo, J.-L., and Prévôt, A. S. H.: Sources of particulate-matter air pollution and its oxidative
712 potential in Europe, *Nature*, 587, 414–419, <https://doi.org/10.1038/s41586-020-2902-8>, 2020.
- 713 Dhalla, N., Temsah, R. M., and Neticadan, Th.: Role of oxidative stress in cardiovascular diseases, *J. Hypertens.*, 18,
714 <https://doi.org/655-673>, 10.1097/00004872-200018060-00002, 2000.
- 715 Dai, Q., Hopke, Ph. K., Bi, X., and Feng, Y.: Improving apportionment of PM_{2.5} using multisite PMF by constraining G-
716 values with a priori information, *Sci. Total Environ.*, 736, 139657, <https://doi.org/10.1016/j.scitotenv.2020.139657>,
717 2020.
- 718 Donaldson, K., Tran, L., Jimenez, L., Duffin, R., Newby, D., Mills, N., MacNee, W., and Stone, V.: Combustion-derived
719 nanoparticles: a review of their toxicology following inhalation exposure, *Part. Fibre Toxicol.*, 2, 10,
720 <https://doi.org/10.1186/1743-8977-2-10>, 2005.
- 721 EPA: Positive matrix factorization model for environmental data analyses, [https://www.epa.gov/air-research/positive-](https://www.epa.gov/air-research/positive-matrix-factorization-model-environmental-data-analyses)
722 [matrix-factorization-model-environmental-data-analyses](https://www.epa.gov/air-research/positive-matrix-factorization-model-environmental-data-analyses), last access: 20 June 2022, 2017.
- 723 Fang, T., Verma, V., Bates, J. T., Abrams, J., Klein, M., Strickland, M. J., Sarnat, S. E., Chang, H. H., Mulholland, J. A.,
724 Tolbert, P. E., Russell, A. G., and Weber, R. J.: Oxidative potential of ambient water-soluble PM_{2.5} in the southeastern
725 United States: contrasts in sources and health associations between ascorbic acid (AA) and dithiothreitol (DTT) assays,
726 *Atmos. Chem. Phys.*, 16, 3865–3879, <https://doi.org/10.5194/acp-16-3865-2016>, 2016.
- 727 Fang, T., Guo, H., Zeng, L., Verma, V., Nenes, A., and Weber, R. J.: Highly acidic ambient particles, soluble metals, and
728 oxidative potential: a link between sulfate and aerosol toxicity, *Environ. Sci. Technol.*, 51, 2611–2620,
729 <https://doi.org/10.1021/acs.est.6b06151>, 2017.
- 730 Furu, E., Angyal, A., Szoboszlai, Z., Papp, E., Török, Z., and Kertész, Z.: Characterization of aerosol pollution in two
731 Hungarian cities in winter 2009–2010, *Atmosphere*, 13, 554, <https://doi.org/10.3390/atmos13040554>, 2022.
- 732 Gao, D., Ripley, S., Weichenthal, S., and Godri Pollitt, K. J.: Ambient particulate matter oxidative potential: chemical
733 determinants, associated health effects, and strategies for risk management, *Free Radic. Biol. Med.*, 151, 7–25,
734 <https://doi.org/10.1016/j.freeradbiomed.2020.04.028>, 2020.
- 735 Godri, K. J., Harrison, R. M., Evans, T., Baker, T., Dunster, C., Mudway, I. S., and Kelly, F. J.: Increased oxidative burden
736 associated with traffic component of ambient particulate matter at roadside and urban background schools sites in
737 London, *PLoS One*, 6, 1–11, <https://doi.org/10.1371/journal.pone.0021961>, 2011.
- 738 Grange, S. K., Uzu, G., Weber, S., Jaffrezo, J.-L., and Hueglin, C.: Linking Switzerland's PM₁₀ and PM_{2.5} oxidative potential
739 (OP) with emission sources, *Atmos. Chem. Phys.*, 22, 7029–7050, <https://doi.org/10.5194/acp-22-7029-2022>, 2022.
- 740 Hoffer, A., Tóth, Á., Jancsek-Turóczi, B., Machon, A., Meiramova, A., Nagy, A., Marmureanu, L., and Gelencsér, A.:
741 Potential new tracers and their mass fraction in the emitted PM₁₀ from the burning of household waste in stoves,
742 *Atmos. Chem. Phys.*, 21, 17855–17864, <https://doi.org/10.5194/acp-21-17855-2021>, 2021.
- 743 Hopke, P. K.: Review of receptor modeling methods for source apportionment, *J. Air. Waste Manag. Assoc.*, 66, 237–259,
744 <https://doi.org/10.1080/10962247.2016.1140693>, 2016.
- 745 Hopke, P. K.: A guide to positive matrix factorization, Clarkon University, Potsdam, USA, 2000.
- 746 In 't Veld, M., Pandolfi, M., Amato, F., Pérez, N., Reche, C., Dominutti, P., Jaffrezo, J.-L., Alastuey, A., Querol, X., and
747 Uzu, G.: Discovering oxidative potential (OP) drivers of atmospheric PM₁₀, PM_{2.5}, and PM₁ simultaneously in North-
748 Eastern Spain, *Sci. Total Environ.*, 857, 159386, <https://doi.org/10.1016/j.scitotenv.2022.159386>, 2023.
- 749 Katerji, M., Filippova, M., and Duerksen-Hughes, P.: Approaches and methods to measure oxidative stress in clinical
750 samples: research applications in the cancer field, *Oxidative Med. Cell. Longev.*, 12, 1279250,
751 <https://doi.org/10.1155/2019/1279250>, 2019.
- 752 Kelly, F. J. and Mudway, I. S.: Protein oxidation at the air-lung interface, *Amino Acids*, 25, 375–396,
753 <https://doi.org/10.1007/s00726-003-0024-x>, 2003.
- 754 Kelly, F. J. and Fussell, J. C.: Size, source and chemical composition as determinants of toxicity attributable to ambient
755 particulate matter, *Atmos. Environ.*, 60, 504–526, <https://doi.org/10.1016/j.atmosenv.2012.06.039>, 2012.
- 756 Kelly, F. J. and Fussell, J. C.: Air pollution and public health: emerging hazards and improved understanding of risk,
757 *Environ. Geochem. Health*, 37, 631–649, <https://doi.org/10.1007/s10653-015-9720-1>, 2015.
- 758 Kelly, F. J. and Fussell, J. C.: Toxicity of airborne particles-established evidence, knowledge gaps and emerging areas of
759 importance, *Philos. Trans. R. Soc.*, A378, 2019.0322, <https://doi.org/10.1098/rsta.2019.0322>, 2020.
- 760 Kodros, J. K., Papanastasiou, D. K., Paglione, M., Masiol, M., Squizzato, S., Florou, K., Skyllakou, K., Kaltsonoudis, Ch.,
761 Nenes, A., and Pandis, S. N.: Rapid dark aging of biomass burning as an overlooked source of oxidized organic aerosol,
762 *Proc. Natl. Acad. Sci. USA*, 117, 33028–33033, <https://doi.org/10.1073/pnas.2010365117>, 2020.



- 763 Kurihara, K., Iwata, A., Murray Horwitz, S. G., Ogane, K., Sugioka, T., Matsuki, A., and Okuda, T.: Contribution of
764 physical and chemical properties to dithiothreitol-measured oxidative potentials of atmospheric aerosol particles at
765 urban and rural sites in Japan, *Atmosphere*, 13, 319, <https://doi.org/10.3390/atmos13020319>, 2022.
- 766 Künzli, N., Mudway, I. S., Gotschi, T., Shi, T. M., Kelly, F. J., Cook, S., Burney, P., Forsberg, B., Gauderman, J. W.,
767 Hazenkamp, M. E., Heinrich, J., Jarvis, D., Norback, D., Payo-Losa, F., Poli, A., Sunyer, J., and Borm, P. J. A.:
768 Comparison of oxidative properties, light absorbance, and total and elemental mass concentration of ambient PM_{2.5}
769 collected at 20 European sites, *Environ. Health Perspect.*, 114, 684–690, <https://doi.org/10.1289/ehp.8584>, 2006.
- 770 Lelieveld, J., Evans, J. S., Fnais, M., Giannadaki, D., Pozzer, A.: The contribution of outdoor air pollution sources to
771 premature mortality on a global scale, *Nature*, 525, 367–371, <https://doi.org/10.1038/nature15371>, 2015.
- 772 Lelieveld, J., Pozzer, A., Pöschl, U., Fnais, M., Haines, A., and Münzel, T.: Loss of life expectancy from air pollution
773 compared to other risk factors: a worldwide perspective, *Cardiovasc. Res.*, 116, 1910–1917,
774 <https://doi.org/10.1093/cvr/cvaa073>, 2020.
- 775 Lionetto, M. G., Guascito, M. R., Giordano, M. E., Caricato, R., De Bartolomeo, A. R., Romano, M. P., Conte, M., Dinoi,
776 A., and Contini, D.: Oxidative potential, cytotoxicity, and intracellular oxidative stress generating capacity of PM₁₀: a
777 case study in south of Italy, *Atmosphere*, 12, 464, <https://doi.org/10.3390/atmos12040464>, 2021.
- 778 Norris, G., Duvall, R., Brown, S., and Bai, S.: EPA Positive Matrix Factorization (PMF) 5.0 fundamentals and user guide,
779 Technical Report, U.S. Environmental Protection Agency, National Exposure Research Laboratory, Washington, USA,
780 2014.
- 781 Paatero, P. and Tapper, U.: Positive matrix factorization: A non-negative factor model with optimal utilization of error
782 estimates of data values, *Environmetrics*, 5, 111–126, <https://doi.org/10.1002/env.3170050203>, 1994.
- 783 Pye, H. O. T., Ward-Caviness, C. K., Murphy, B. N., Appel, K. W., and Seltzer, K. M.: Secondary organic aerosol
784 association with cardiorespiratory disease mortality in the United States, *Nat. Commun.*, 12, 7215,
785 <https://doi.org/10.1038/s41467-021-27484-1>, 2021.
- 786 Riediker, M., Zink, D., Kreyling, W., Oberdörster, G., Elder, A., Graham, U., Lynch, I., Duschl, A., Ichihara, G., Ichihara,
787 S., Kobayashi, T., Hisanaga, N., Umezawa, M., Cheng, T. J., Handy, R., Gulumian, M., Tinkle, S., and Cassee, F.:
788 Particle toxicology and health - where are we?, *Part. Fibre Toxicol.*, 16, 19, <https://doi.org/10.1186/s12989-019-0302-8>,
789 2019.
- 790 Salma, I., Chi, X., and Maenhaut, W.: Elemental and organic carbon in urban canyon and background environments in
791 Budapest, Hungary, *Atmos. Environ.*, 38, 27–36, <https://doi.org/10.1016/j.atmosenv.2003.09.047>, 2004.
- 792 Salma, I., Ocskay, R., Raes, N., and Maenhaut, W.: Fine structure of mass size distributions in urban environment, *Atmos.*
793 *Environ.*, 39, 5363–5374, <https://doi.org/10.1016/j.atmosenv.2005.05.021>, 2005.
- 794 Salma, I. and Maenhaut, W.: Changes in chemical composition and mass of atmospheric aerosol pollution between 1996 and
795 2002 in a Central European city, *Environ. Pollut.*, 143, 479–488, <https://doi.org/10.1016/j.envpol.2005.11.042>, 2006.
- 796 Salma, I., Németh, Z., Weidinger, T., Kovács, B., and Kristóf, G.: Measurement, growth types and shrinkage of newly
797 formed aerosol particles at an urban research platform, *Atmos. Chem. Phys.*, 16, 7837–7851,
798 <https://doi.org/10.5194/acp-16-7837-2016>, 2016.
- 799 Salma, I., Vasanits-Zsigrai, A., Machon, A., Varga, T., Major, I., Gergely, V., and Molnár, M.: Fossil fuel combustion,
800 biomass burning and biogenic sources of fine carbonaceous aerosol in the Carpathian Basin, *Atmos. Chem. Phys.*, 20,
801 4295–4312, <https://doi.org/10.5194/acp-20-4295-2020>, 2020a.
- 802 Salma, I., Vörösmarty, M., Gyöngyösi, A. Z., Thén, W., and Weidinger, T.: What can we learn about urban air quality with
803 regard to the first outbreak of the COVID-19 pandemic? A case study from central Europe, *Atmos. Chem. Phys.*, 20,
804 15725–15742, <https://doi.org/10.5194/acp-20-15725-2020>, 2020b.
- 805 Salma, I., Varga, P. T., Vasanits, A., Machon, A.: Secondary organic carbon and its contributions in different atmospheric
806 environments of a continental region and seasons, *Atmos. Res.*, 278, 106360,
807 <https://doi.org/10.1016/j.atmosres.2022.106360>, 2022.
- 808 Shahpoury, P., Zhang, Z. W., Arangio, A., Celo, V., Dabek-Zlotorzynska, E., Harner, T., and Nenes, A.: The influence of
809 chemical composition, aerosol acidity, and metal dissolution on the oxidative potential of fine particulate matter and
810 redox potential of the lung lining fluid, *Environ. Internat.*, 148, 106343, <https://doi.org/10.1016/j.envint.2020.106343>,
811 2021.
- 812 Srivastava, D., Tomaz, S., Favez, O., Lanzafame, G. M., Golly, B., Besombes, J.-L., Alleman, L. Y., Jaffrezo, J.-L., Jacob,
813 V., Perraudin, E., Villenave, E., and Albinet, A.: Speciation of organic fraction does matter for source apportionment.
814 Part I: A one-year campaign in Grenoble (France), *Sci. Total Environ.*, 624, 1598–1611,
815 <https://doi.org/10.1016/j.scitotenv.2017.12.135>, 2018.



- 816 Szigeti, T., Óvári, M., Dunster, C., Kelly, F. J., Lucarelli, F., and Zárny, G.: Changes in chemical composition and oxidative
817 potential of urban PM_{2.5} between 2010 and 2013 in Hungary, *Sci. Total Environ.*, 518–519, 534–544,
818 <https://doi.org/10.1016/j.scitotenv.2015.03.025>, 2015.
- 819 Valavanidis, A., Fiotakis, K., and Vlachogianni, T.: Airborne particulate matter and human health: toxicological assessment
820 and importance of size and composition of particles for oxidative damage and carcinogenic mechanisms, *J. Environ.*
821 *Sci. Health C*, 26, 339–362, <https://doi.org/10.1080/10590500802494538>, 2008.
- 822 Valavanidis, A., Vlachogianni, T., Fiotakis, K., and Loridas, S.: Pulmonary oxidative stress, inflammation and cancer:
823 respirable particulate matter, fibrous dusts and ozone as major causes of lung carcinogenesis through reactive oxygen
824 species mechanisms, *Int. J. Environ. Res. Public Health*, 10, 3886–3907, <https://doi.org/10.3390/ijerph10093886>, 2013.
- 825 Varga, G.: Changing nature of Saharan dust deposition in the Carpathian Basin (Central Europe): 40 years of identified
826 North African dust events (1979–2018), *Environ. Int.*, 139, 105712, <https://doi.org/10.1016/j.envint.2020.105712>,
827 2020.
- 828 Verma, V., Rico-Martinez, R., Kotra, N., King, L., Liu, J., Snell, T. W., and Weber, R. J.: Contribution of water-soluble and
829 insoluble components and their hydrophobic/hydrophilic subfractions to the reactive oxygen species-generating
830 potential of fine ambient aerosols, *Environ. Sci. Technol.*, 46, 11384–11392, <https://doi.org/10.1021/es302484r>, 2012
- 831 Verma, V., Fang, T., Guo, H., King, L., Bates, J. T., Peltier, R. E., Edgerton, E., Russell, A. G., and Weber, R. J.: Reactive
832 oxygen species associated with water-soluble PM_{2.5} in the southeastern United States: spatiotemporal trends and source
833 apportionment, *Atmos. Chem. Phys.*, 14, 12915–12930, <https://doi.org/10.5194/acp-14-12915-2014>, 2014.
- 834 Verma, V., Fang, T., Xu, L., Peltier, R. E., Russell, A. G., Ng, N. L., and Weber, R. J.: Organic aerosols associated with the
835 generation of reactive oxygen species (ROS) by water-soluble PM_{2.5}, *Environ. Sci. Technol.*, 49, 4646–4656,
836 <https://doi.org/10.1021/es505577w>, 2015.
- 837 Visentin, M., Pagnoni, A., Sarti, E., and Pietrogrande, M. C.: Urban PM_{2.5} oxidative potential: Importance of chemical
838 species and comparison of two spectrophotometric cell-free assays, *Environ. Pollut.*, 219, 72–79,
839 <https://doi.org/10.1016/j.envpol.2016.09.047>, 2016.
- 840 Wang, S., Ye, J., Soong, R., Wu, B., Yu, L., Simpson, A. J., and Chan, A. W. H.: Relationship between chemical
841 composition and oxidative potential of secondary organic aerosol from polycyclic aromatic hydrocarbons, *Atmos.*
842 *Chem. Phys.*, 18, 3987–4003, <https://doi.org/10.5194/acp-18-3987-2018>, 2018.
- 843 Weber, S., Uzu, G., Calas, A., Chevrier, F., Besombes, J.-L., Charron, A., Salameh, D., Ježek, I., Močnik, G., and Jaffrezo,
844 J.-L.: An apportionment method for the oxidative potential of atmospheric particulate matter sources: application to a
845 one-year study in Chamonix, France, *Atmos. Chem. Phys.*, 18, 9617–9629, <https://doi.org/10.5194/acp-18-9617-2018>,
846 2018.
- 847 Weber, S., Uzu, G., Favez, O., Borlaza, L. J. S., Calas, A., Salameh, D., Chevrier, F., Allard, J., Besombes, J.-L., Albinet, A.,
848 Pontet, S., Mesbah, B., Gille, G., Zhang, S., Pallares, C., Leoz-Garziandia, E., and Jaffrezo, J.-L.: Source
849 apportionment of atmospheric PM₁₀ oxidative potential: synthesis of 15 year-round urban datasets in France, *Atmos.*
850 *Chem. Phys.*, 21, 11353–11378, <https://doi.org/10.5194/acp-21-11353-2021>, 2021.
- 851 Wong, J. P. S., Tsagkarakaki, M., Tsiodra, I., Mihalopoulos, N., Violaki, K., Kanakidou, M., Sciare, J., Nenes, A., and Weber,
852 R. J.: Effects of atmospheric processing on the oxidative potential of biomass burning organic aerosols, *Environ. Sci.*
853 *Technol.*, 53, 6747–6756, <https://doi.org/10.1021/acs.est.9b01034>, 2019.
- 854 Yang, A., Hellack, B., Leseman, D., Brunekreef, B., Kuhlbusch, T. A., Cassee, F. R., Hoek, G., and Janssen, N. A.:
855 Temporal and spatial variation of the metal-related oxidative potential of PM_{2.5} and its relation to PM_{2.5} mass and
856 elemental composition, *Atmos. Environ.*, 102, 62–69, <https://doi.org/10.1016/j.atmosenv.2014.11.053>, 2015.
- 857 Yu, S., Liu, W., Xu, Y., Yi, K., Zhou, M., Tao, S., and Liu, W.: Characteristics and oxidative potential of atmospheric PM_{2.5}
858 in Beijing: Source apportionment and seasonal variation, *Sci. Total Environ.*, 650, 277–287,
859 <https://doi.org/10.1016/j.scitotenv.2018.09.021>, 2019.
- 860 Yue, Y., Chen, H., Setyan, A., Elser, M., Dietrich, M., Li, J., Zhang, T., Zhang, X., Zheng, Y., Wang, J., and Yao, M.: Size-
861 resolved endotoxin and oxidative potential of ambient particles in Beijing and Zürich, *Environ. Sci. Technol.*, 52,
862 6816–6824, <https://doi.org/10.1021/acs.est.8b01167>, 2018.
- 863 Zhang, Z.-H., Hartner, E., Utinger, B., Gfeller, B., Paul, A., Sklorz, M., Czech, H., Yang, B. X., Su, X. Y., Jakobi, G.,
864 Orasche, J., Schnelle-Kreis, J., Jeong, S., Gröger, T., Pardo, M., Hohaus, T., Adam, T., Kiendler-Scharr, A., Rudich, Y.,
865 Zimmermann, R., and Kalberer, M.: Are reactive oxygen species (ROS) a suitable metric to predict toxicity of
866 carbonaceous aerosol particles?, *Atmos. Chem. Phys.*, 22, 1793–1809, <https://doi.org/10.5194/acp-22-1793-2022>, 2022.